NASA TECHNICAL MEMORANDUM

NASA TM X-2602

NASA TM X-2602

INITIAL DEVELOPMENT OF A HYPERSONIC FREE MIXING LAYER

by William D. Harvey and Robert L. Bolton

Langley Research Center
Hampton, Va. 23365

NATIONAL AERONAUTICS AND SPACE ADMINISTRATION • WASHINGTON, D. C. • OCTOBER 1972

1. Report No.	2. Government Accession No.	3. Recipient's Catalog No.
NASA TM X-2602		

4. Title and Subtitle	5. Report Date
INITIAL DEVELOPMENT OF A HYPERSONIC FREE MIXING LAYER	October 1972
	6. Performing Organization Code
7. Author(s)	8. Performing Organization Report No.
William D. Harvey and Robert L. Bolton	L-8409
	10. Work Unit No.
9. Performing Organization Name and Address	501-06-08-01
NASA Langley Research Center Hampton, Va. 23365	11. Contract or Grant No.
	13. Type of Report and Period Covered
12. Sponsoring Agency Name and Address	Technical Memorandum
National Aeronautics and Space Administration Washington, D.C. 20546	14. Sponsoring Agency Code

15. Supplementary Notes

16. Abstract

A preliminary experimental investigation to establish some of the characteristics and further the understanding of the initial development of a turbulent free mixing layer for hypersonic speeds has been conducted. Mean profile data at about 15 centimeters (6 inches) downstream of the exit of a hypersonic nozzle have been obtained in nitrogen for a nominal Mach number of 19.5, total temperature of about 1670° K (3000° R), and Reynolds number range from about 1.6×10^6 to 3.6×10^6 per meter (5×10^5 to 11×10^5 per foot) and have been compared with profiles upstream of the nozzle exit. Static pressure varied across the shear layer for the present tests. The outer 80 percent of the high-velocity portion of the free shear layer can be calculated by a rotational method of characteristics. However, turbulent mixing is evidently important in the low-velocity region, and effects of eddy viscosity and eddy conductivity should be included in a theoretical analysis.

17. Key Words (Suggested by Author(s))	18. Distribution Statement
Shear layer Hypersonic nozzle Turbulent flow	Unclassified – Unlimited

19. Security Classif. (of this report)	20. Security Classif. (of this page)	21. No. of Pages	22. Price*
Unclassified	Unclassified	22	$3.00

*For sale by the National Technical Information Service, Springfield, Virginia 22151

INITIAL DEVELOPMENT OF A HYPERSONIC FREE MIXING LAYER

By William D. Harvey and Robert L. Bolton
Langley Research Center

SUMMARY

A preliminary experimental investigation to establish some of the characteristics and further the understanding of the initial development of a turbulent free mixing layer for hypersonic speeds has been conducted. Mean profile data at about 15 centimeters (6 inches) downstream of the exit of a hypersonic nozzle have been obtained in nitrogen for a nominal Mach number of 19.5, total temperature of about 1670° K (3000° R), and Reynolds number range from about 1.6×10^6 to 3.6×10^6 per meter (5×10^5 to 11×10^5 per foot) and have been compared with profiles upstream of the nozzle exit. Static pressure varied across the shear layer for the present tests. The outer 80 percent of the high-velocity portion of the free shear layer can be calculated by a rotational method of characteristics. However, turbulent mixing is evidently important in the low-velocity region, and effects of eddy viscosity and eddy conductivity should be included in a theoretical analysis.

INTRODUCTION

The study of turbulent free mixing layers relates to problems associated with wakes of high-speed missiles and reentry vehicles, base injection, exhaust plumes, and supersonic combustion. Experimental data (refs. 1 to 3) and theoretical methods of analysis (refs. 4 to 7) are available for supersonic free jets. However, no data on the initial development of a hypersonic turbulent free mixing layer are available. Preliminary results are reported herein of an experimental investigation to establish some of the characteristics of turbulent free mixing at hypersonic speeds.

SYMBOLS

Values are given in both SI and U.S. Customary Units. The measurements and calculations were made in U.S. Customary Units.

D	diameter
M	Mach number
N_{Re}/m	unit Reynolds number, $\rho u/\mu$, per meter
N_{Re}/ft	unit Reynolds number, $\rho u/\mu$, per foot
$N_{Re,x}$	local Reynolds number based on streamwise distance from flow origin
p	pressure
p_{t_2}	pitot pressure
T	temperature
u	velocity
x	downstream distance from nozzle throat
y	normal distance from centerline
y_δ	distance from centerline to shear layer or boundary-layer edge as indicated by pitot profiles
μ	viscosity
ρ	density

Subscripts:

B	test box
e	edge conditions
o	total conditions
t	local total conditions

W nozzle wall

A bar over a symbol denotes mean value.

APPARATUS AND TESTS

A schematic drawing of the Langley hypersonic nitrogen tunnel and test equipment used in the experiment is shown in figure 1. A description of the facility and its

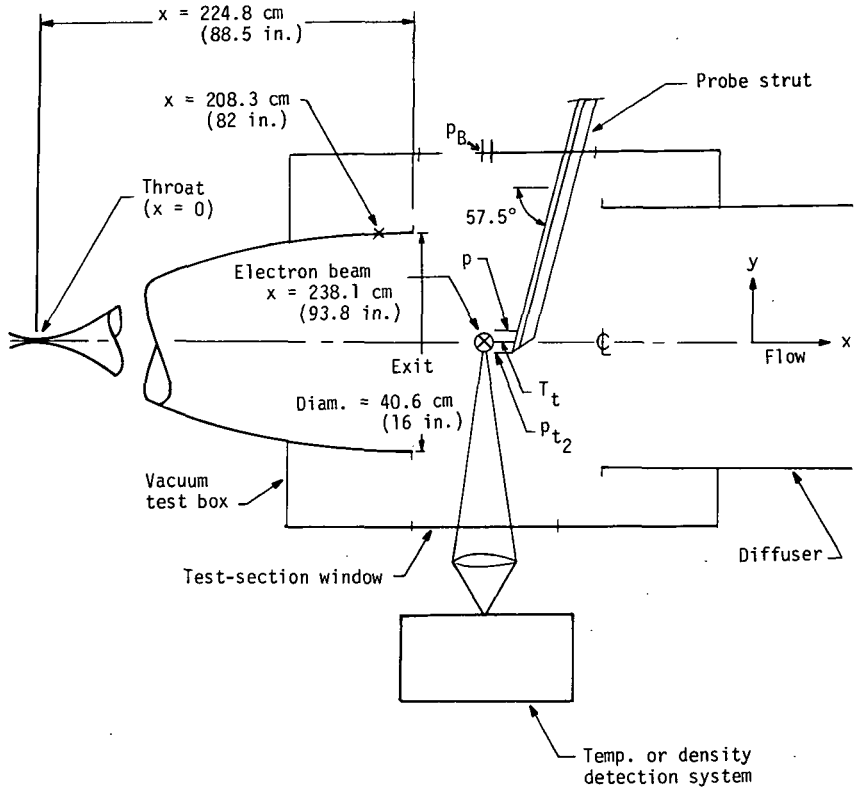

Figure 1.- Schematic drawing of facility and test apparatus.

operation and preliminary calibrations of the flow are presented in reference 8. The facility can be operated continuously for run times in excess of 2 hours. The boundary layer at the exit (x = 224.8 cm (88.5 in.) downstream of the throat) of the nozzle is approximately 10 cm (4 in.) thick (ref. 9).

Detailed surveys of mean total temperature, pitot pressure, and static pressure were made with probes across the initial shear layer region at x = 238.1 cm (93.8 in.) or about 1.5 boundary-layer thicknesses downstream of the nozzle exit. The electron beam technique was also utilized to measure the mean density and static temperature.

Probe survey data were previously obtained in the turbulent boundary layer on the nozzle wall at station x = 208.3 cm (82 in.) (ref. 9), and representative profiles are included herein for comparison with the present data. Actual stagnation and test conditions are given in table I. Tests were made at a nominal Mach number of 19.5 in high purity nitrogen (five parts per million of oxygen impurities) at a nominal total temperature of about 1670° K (3000° R). The jet free-stream Reynolds number was varied from 1.6×10^6 to 3.6×10^6 per meter (5×10^5 to 11×10^5 per foot). In this free mixing problem, the jet free stream is defined as being the inviscid flow region along the nozzle or jet centerline.

INSTRUMENTATION AND DATA REDUCTION

The survey probes and water-cooled strut were located on the opposite side of the tunnel from the electron beam density or temperature apparatus as shown in figure 1. Pitot probes were made of stainless steel tubes with an external diameter of 0.318 cm (0.125 in.). The static-pressure probe was a cone cylinder with 0.079-cm-diameter (0.031-inch-diameter) orifices located 90° apart on the 0.318-cm-diameter (0.125-inch-diameter) cylinder, 5.08 cm (2 in.) downstream of the cone tip. Detailed sketches of the probes are included in subsequent figures. Absolute pressure transducers were used to measure both the pitot and static pressures. The data from both pressure probes have been analyzed for viscous and rarefaction effects and corrections have been applied. Reference 9 gives a detailed description of these correction procedures and of the instrumentation and probes.

The total-temperature probe was an alumel bare wire of 0.0254-cm (0.01-in.) diameter placed normal to the flow, with small chromel wires of 0.00762-cm (0.003-in.) diameter attached to the center and at the ends. The small chromel wires attached to the ends of the alumel wire enabled the evaluation of heat conduction losses. The chromel wire attached to the center measured the temperature at the center point of symmetry of the probe. This measured temperature was then corrected for both radiation and conduction losses by using the method of reference 10. The total temperature through the shear layer varied considerably from approximately 1670° K (3000° R) down to 333° K (600° R). Therefore, measured values of emittance over a wide temperature range for alumel wire (ref. 9) were used in the present data reduction procedure for the temperature probe. In general, the maximum correction to the measured total temperature occurred in the jet free stream and amounted to about 20 percent. Experimental values of pitot and total temperature for the probes are given in table II. The values given in the table include all corrections previously discussed. The use of real gas properties was found to affect computed flow properties only a few percent.

The electron beam gun, mounted on top of the tunnel in the vertical center plane, was operated at a potential difference of about 25 kilovolts with a beam current of about 500 microamperes. The beam direction is normal to both the flow direction and the optical axis of the detection system. (See fig. 1.) A detailed discussion of the electron beam and associated instrumentation used for similar measurements may be found in reference 11. Measurements through the shear layer and free stream were made by remotely traversing the density or temperature apparatus in the vertical direction parallel to the beam.

The density detector system consisted of a photomultiplier tube and interference filter (3914 Å with a width of 30 Å) which observed the fluorescence from the first negative system, (0-0) vibrational band, of the N_2^+ excitation. The detector, with a magnification factor of 0.5, views a cylindrical sample volume of the beam determined by the slit height along the beam and the diameter of the beam. The slit height was 0.159 cm (0.0625 in.) and the slit width (perpendicular to beam axis) was 5.1 cm (2 in.). Owing to beam spreading in the jet free stream, a wide slit was necessary to insure collection of all fluorescence from the sample volume for absolute density measurements. The sample volume was about 0.0016 cu cm (0.0001 cu in.) in the vicinity of the drift tube (beam source) and became progressively larger with increasing distance from the drift tube (toward the free stream).

The rotational temperature measurements (ref. 12) were made with a 0.5-meter Ebert-Fastie scanning spectrometer and photomultiplier detector. The slit dimensions were 30 μm by 0.5 cm with the longest dimension along the axis of the beam.

THEORY

As the nozzle-wall boundary layer leaves the exit, the shear stress near the low-velocity edge of the free shear layer rapidly decreases in magnitude with increasing downstream distance. The outer portion, or high-velocity region, of the shear layer will also have small shear owing to the small values of velocity gradient. Hence, the flow in this region is assumed to be essentially an inviscid rotational flow field (ref. 13). In order to determine whether the present shear profiles are representative of an inviscid rotational flow field, the experimental velocity and Mach number profiles are compared with theoretical profiles by using the method of reference 14. The computer program of reference 14 calculates nonuniform supersonic flows by a viscous characteristic method, in which the transport properties are assumed to be functions only of gradients normal to the streamlines. The initial program input profile of Mach number, velocity, and static pressure perpendicular to the nozzle centerline applies only to the supersonic portion of the flow.

The experimental Mach number and velocity profile obtained at station x = 208.3 cm (82.0 in.) (ref. 9) were scaled to a corresponding boundary-layer thickness at the nozzle exit station x = 224.8 cm (88.5 in.), and used to define conditions on the starting line. The flow was turned 2° at the nozzle exit to correspond approximately to the measured reduction in pressure from p_W at the nozzle exit to p_B in the test chamber. The free-stream Mach number, temperature, and $N_{Re,x}$ were 19.42, 23.3° K (42° R), and 5.9×10^6, respectively, for a nozzle radius of 20.3 cm (8.00 in.). The calculations assumed laminar viscosity and the Prandtl number and Lewis numbers were unity. The initial static-pressure profiles used were either equal to the edge value or a ramp distribution. (See eq. (1) of ref. 9.) Additional calculations (ref. 14) with zero viscosity input gave profiles essentially the same as those computed with laminar viscosity.

RESULTS AND DISCUSSION

Measured values of mean density and mean static temperature through the shear layer from the electron beam are given in table III and are shown in figures 2 and 3, respectively, as the solid symbols. The data are compared with values (open symbols) of

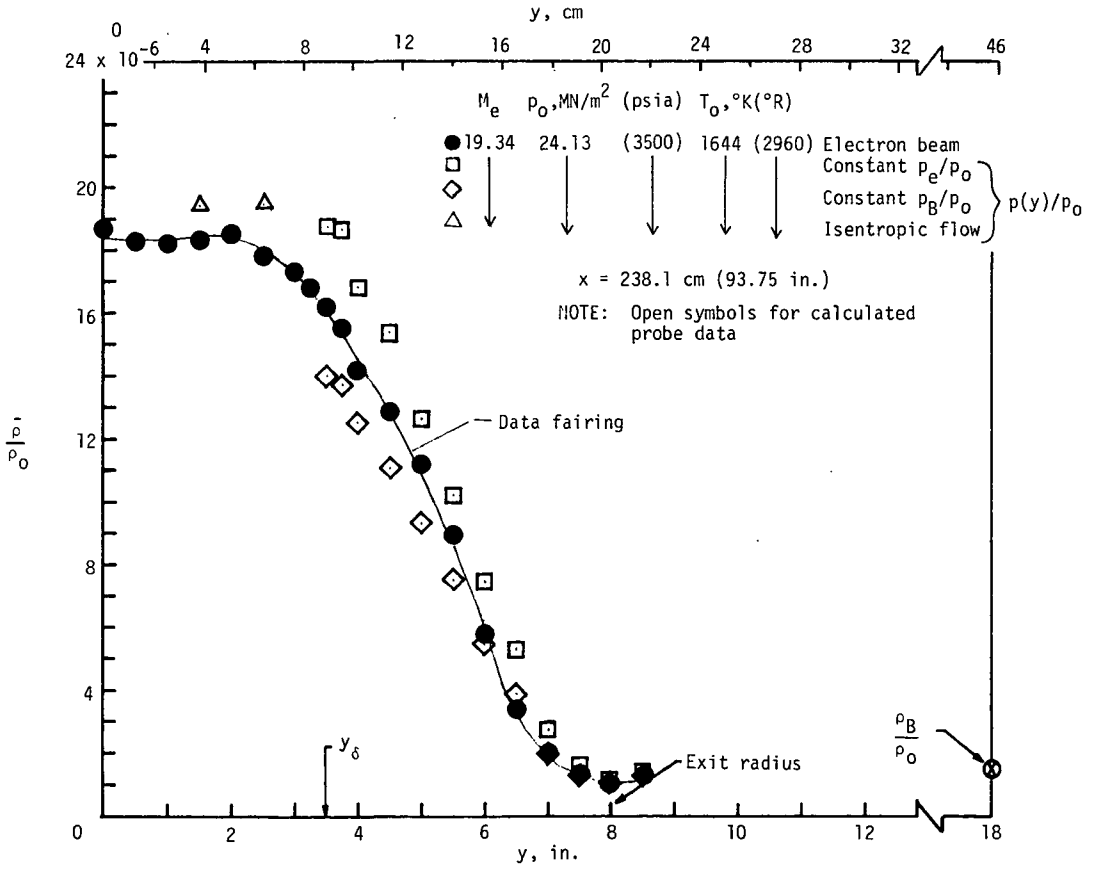

Figure 2.- Mean density through shear layer from electron beam compared with calculated density from probe data.

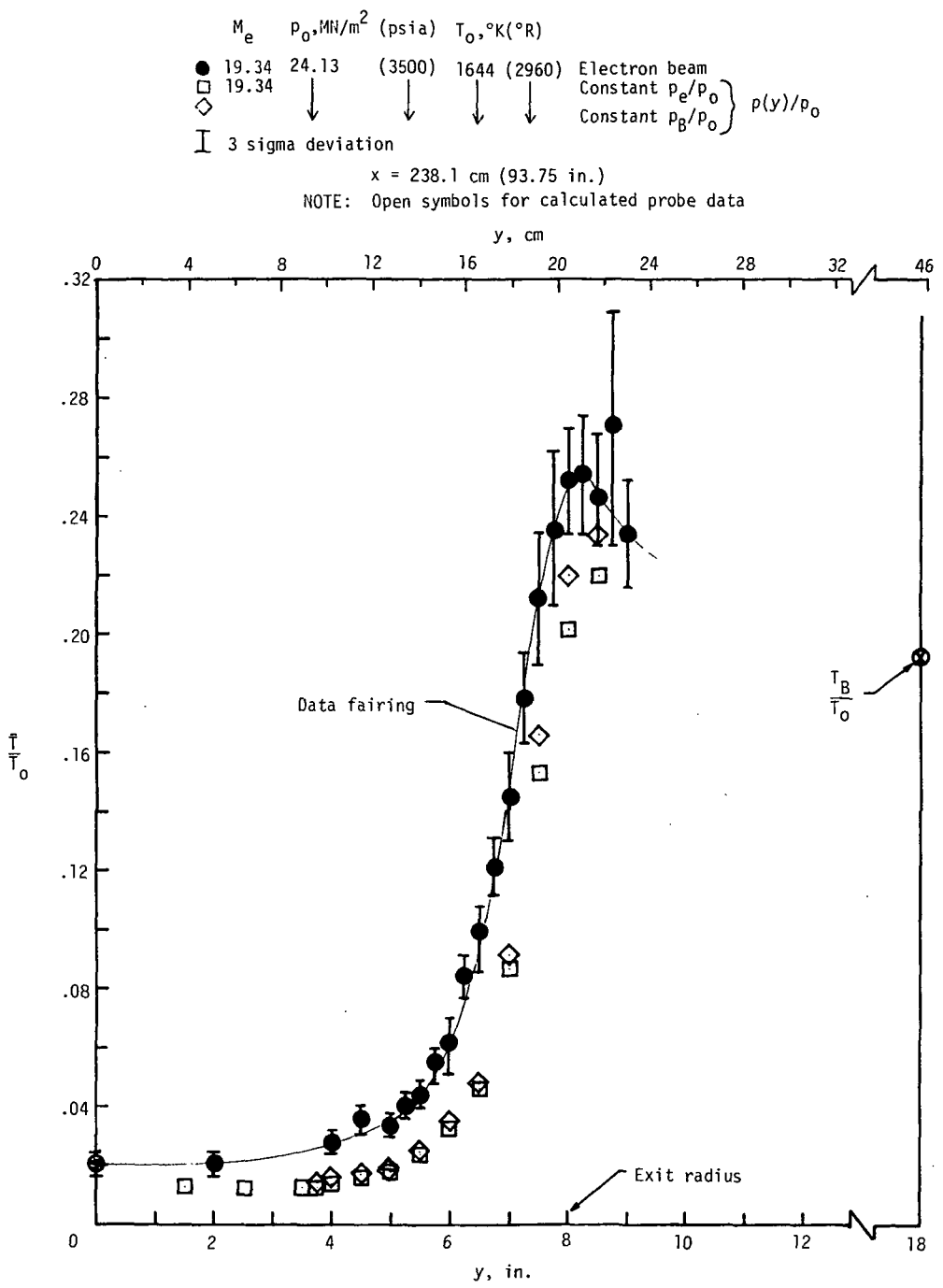

Figure 3.- Static temperature through shear layer from electron beam compared with calculated values from probe data.

density (fig. 2) and temperature (fig. 3) calculated such that $p(y)/p_o = p_e/p_o$ or p_B/p_o through the shear layer along with measured pitot- and total-temperature distributions (figs. 4 and 5). The static pressure p_e corresponds to M_e determined from the pitot profiles (fig. 4) at the shear layer edge.

The comparisons (fig. 2) indicate densities obtained from the electron beam are below those from the probe data based on $p(y)/p_o = p_e/p_o$ and above the probe data for the assumed $p(y)/p_o = p_B/p_o$. The largest disagreements between calculated and electron beam data occur at the higher densities or near free-stream conditions where the temperatures (fig. 3) are the lowest. For such conditions, errors in the measured electron beam density are due to unknown effects of quenching at the higher densities and lower static temperatures. An investigation of this latter effect, reported in reference 15, indicates that apparent quenching increases at low static temperatures and high densities. At the low-density levels encountered through the shear layer (fig. 2) calibrations show that the density varies almost linearly with the fluorescence output and no corrections were applied to account for quenching.

Trends in the temperature distributions calculated from probe data are similar to those from the electron beam (fig. 3) but the probe data are always lower in magnitude. Similar trends in beam temperature data have previously been reported (ref. 16). The electron beam data shown in figure 3 indicate a peak in temperature and a minimum in $\bar{\rho}/\rho_o$ (fig. 2) located near $y \cong 20.32$ cm (8 in.).

Experimental distributions of pitot and static pressures through the shear layer and inviscid flow core are shown in figure 4 for a range of test conditions and survey stations. Average values of test-box pressure p_B/p_o ($x = 250.2$ cm (98.5 in.); $y = 45.72$ cm (18 in.)) and nozzle-wall pressure p_W/p_o ($x = 208.3$ cm (82 in.); $y = 19.69$ cm (7.75 in.)) are included in the figure along with static-pressure values p_e/p_o at the shear layer edge and used to obtain density in figure 2. The nozzle-wall and test-box pressures varied about ±2 percent during the tests. The profiles shown for station $x = 208.3$ cm (82 in.) were obtained previously (ref. 9) on the nozzle wall and are included for comparison. The static-pressure values were obtained from the electron beam measurements of density and temperature with the equation of state

$$\bar{p}/p_o = \left(\bar{\rho}/\rho_o\right)\left(\overline{T}/T_o\right) \tag{1}$$

The curves faired through the data of figures 2 and 3 were used for this purpose. Since the data shown in figures 2 and 3 were not simultaneously obtained, they have been normalized respectively to account for any variations in test conditions for comparison herein.

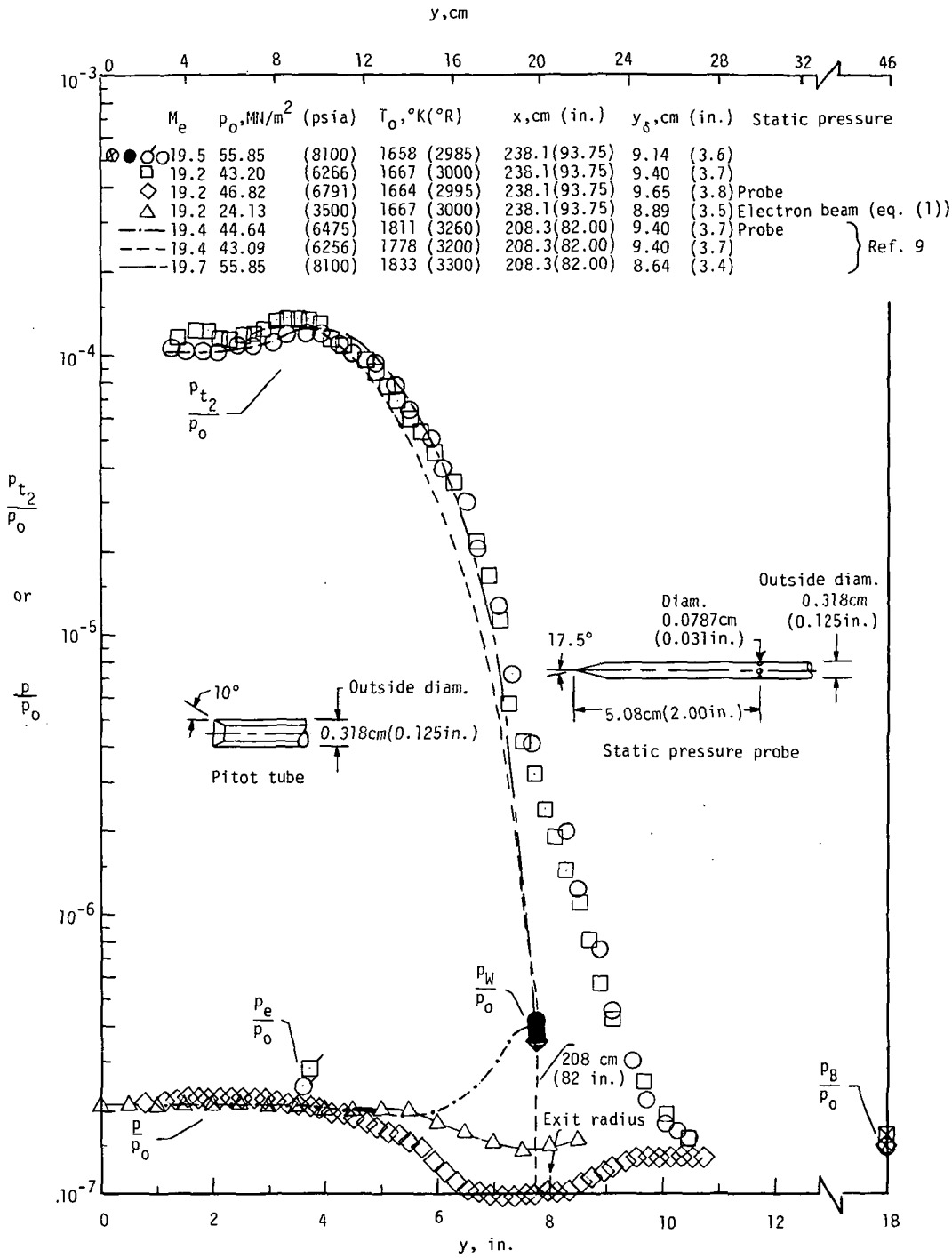

Figure 4.- Impact and static pressure through shear layer downstream of nozzle exit.

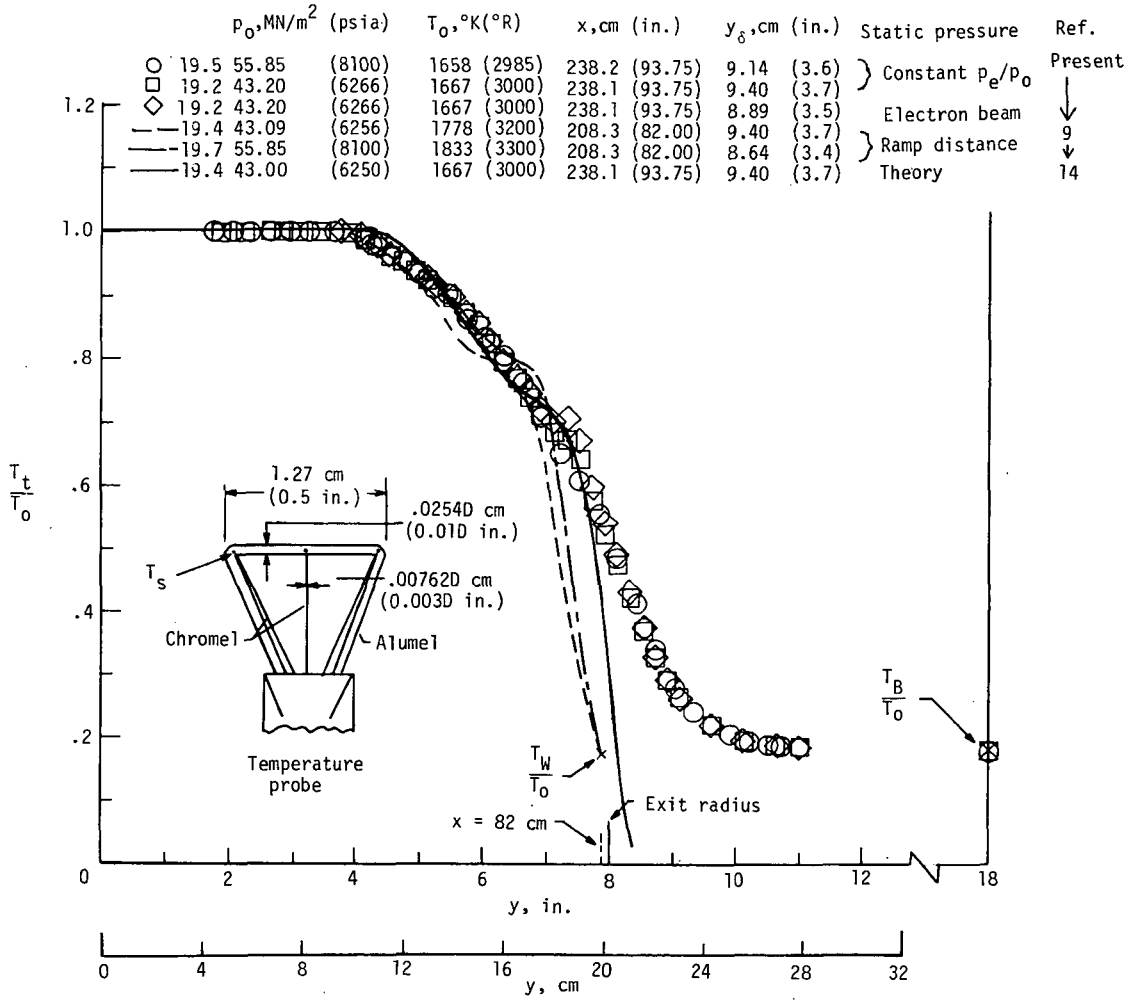

Figure 5.- Comparison of total-temperature distribution through shear layer with theory and with upstream nozzle-wall profiles.

The pitot-pressure profiles at both test stations are nearly the same in the outer boundary-layer region $2.5 \lessapprox y \lessapprox 15$ cm $(1 \lessapprox y \lessapprox 6$ in.). However, some spreading of the flow is evident downstream of the nozzle exit for $y > 18$ cm ($y > 7.0$ in.).

The static-pressure data from the electron beam and from the survey probe indicate that a difference in pressure level exists between the free stream and test box. Variations in static pressure across the shear layer similar to that of the present data have been observed for a Mach 2.6 free jet flow (ref. 1). Differences in magnitude between free-stream, nozzle-wall, and test-box static pressure are also observed for these tests (fig. 4). An overpressure exists between the nozzle wall and test box $p_W/p_B > 1$, thereby indicating a possible expansion at the exit. The static probe pressure in the shear layer falls below the test-box pressure at about $y \cong 14$ cm (5.5 in.). It has been observed previously and suggested in reference 17 that this drop in static

pressure below box pressure with increasing distance from the tunnel centerline may be attributed to effects of the outward expansion of the jet stream and induction of the surrounding fluid. If the induction effect becomes the stronger, the minimum in static pressure would probably move inward toward the flow core with increasing downstream distance. An alternate consideration would be that there is an overexpansion at the nozzle exit causing a reduction in static pressure below the test-box pressure with a recompression to box pressure with increasing static probe distance. No assessment of turbulent effects on the static-pressure readings was made, but it is not expected to alter the overall shape of the data trend.

In comparing the static-pressure probe measurements with the beam results, consideration should be given to the accuracy involved in measuring and correcting static probe pressures at hypersonic speeds (ref. 9) and their use in data reduction procedures. Static-pressure probe corrections were about 50 percent in the free stream and negligible as the probe approached the test-box wall. The electron beam technique provides data (temperature and density) free of interference effects and if no corrections are required for quenching at high density (low temperature) as assumed for the present tests, the resulting values of static pressure should be more reliable than probe data. The uncertainty in temperature measurement was estimated to be about ±20 percent at the low temperatures in the free stream and about ±8 percent near the inner edge of the flow (fig. 3). The uncertainty in the density measurements was estimated to be about ±5 percent at low densities and ±15 percent at high densities. The preceding percentages quoted for the electron beam are for a standard deviation of 3 sigma.

Total-temperature data through the shear layer are compared with nozzle-wall profiles (ref. 9) in figure 5. The experimental temperature data have been reduced for both a constant $p(y)/p_o = p_e/p_o$ or the static pressure from the electron beam data (fig. 4). Also included is the total-temperature profile from the theoretical calculation by the method of reference 14. The theory applies to a ramp-type pressure input (eq. (1) of ref. 9); however, the use of either a constant or a ramp-type distribution of pressure had only a small effect on the computed temperature profile shape. For $y < 18$ cm ($y < 7$ in.), the shear-layer data are similar to the nozzle-wall boundary-layer data as previously observed for the pitot profile data (fig. 4). The agreement of data with theory (fig. 5) indicates that the outer portion $y < 19$ cm ($y < 7.5$ in.) of the temperature profile is representative of an inviscid rotational flow field.

Mach number and velocity profiles (see table IV for values) calculated with either constant p_e/p_o or the electron beam results for p/p_o (not given in table IV) are shown in figures 6(a) and 6(b), respectively. Also shown are upstream nozzle-wall profiles and the calculated Mach number (fig. 6(a)) and velocity (fig. 6(b)) profiles obtained from the

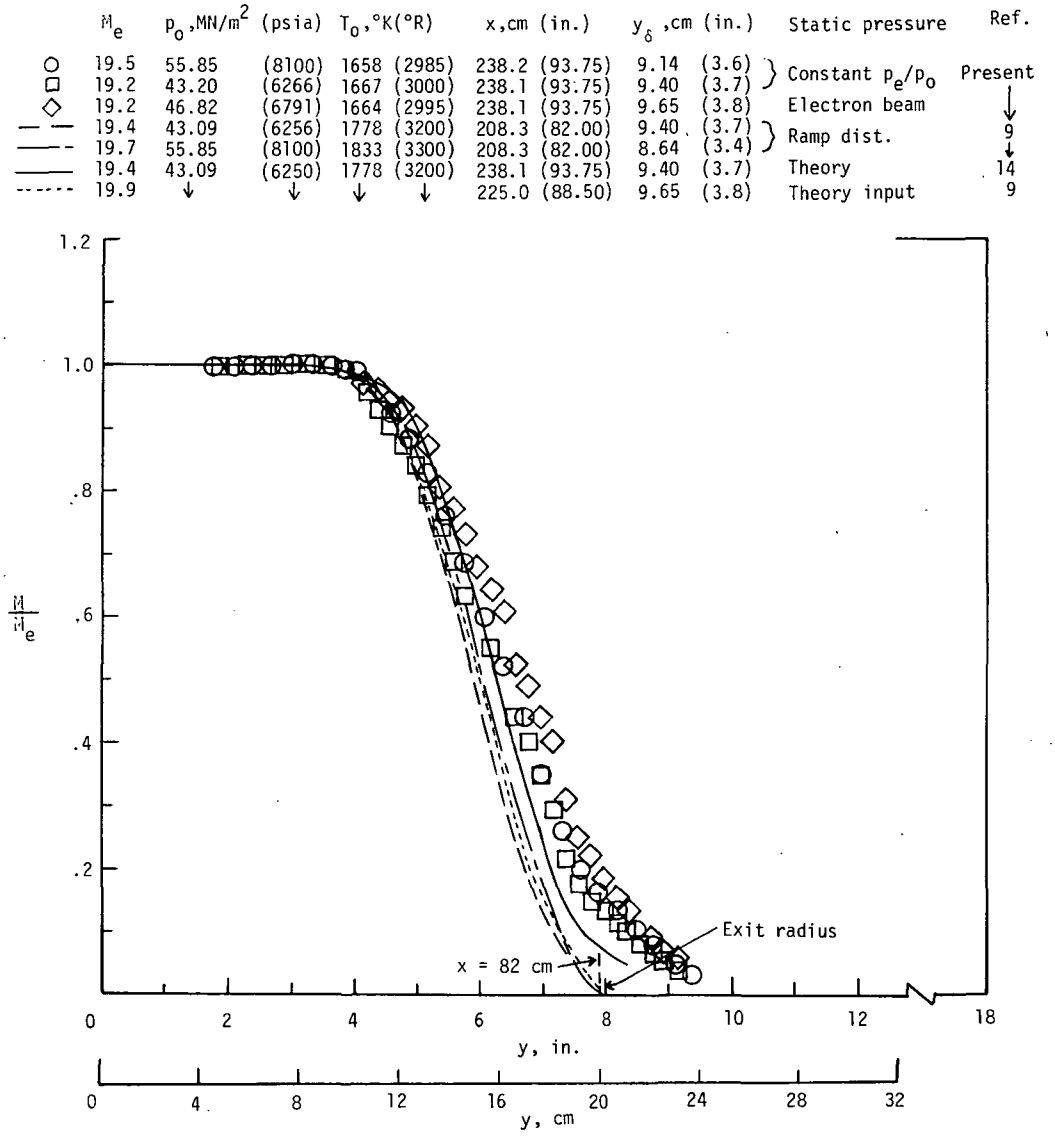

(a) Mach number distribution.

Figure 6.- Comparison of shear flow profiles with theory and with upstream nozzle-wall profiles.

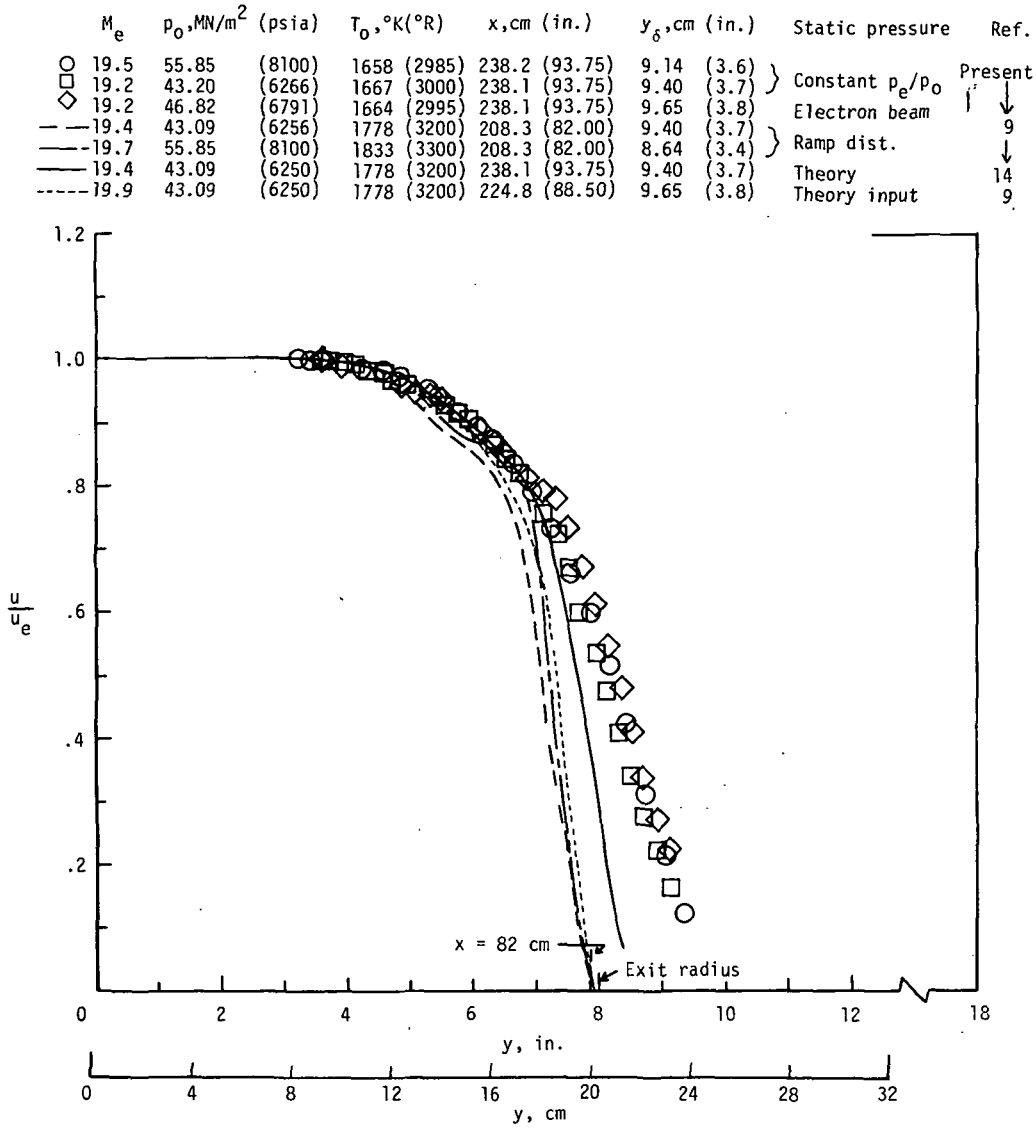

(b) Velocity distribution.

Figure 6.- Concluded.

theory of reference 14 by using a ramp-type pressure input (eq. (1) of ref. 9). Calculations were also made by using a constant value of pressure p_e, and the difference in the velocity and Mach number profiles, compared with a ramp-type pressure input, was a maximum of 0.3 percent and 0.45 percent, respectively, at $y = 20.4$ cm (8.0 in.). The input profiles of Mach number (fig. 6(a)) and velocity (fig. 6(b)) are shown for comparison with the expanded profile.

The negligible difference between experimental velocity profiles and theory out to about $y = 15$ cm (6 in.) (fig. 6(a)) and $y = 18$ cm (7 in.) (fig. 6(b)) shows that, in the short x-distance from 208.28 to 238.125 cm (82 to 93.75 in.), there is little effect of shear in the outer 80 percent of the high-velocity portion of the flow which may be computed by the rotational method of characteristics of reference 14. For values of $y > 15$ or 18 cm (6 or 7 in.), the effects of turbulent mixing are evidently important and should be included in the theory. Note that much larger Reynolds numbers, based on shear layer length, would be required above the present test conditions for the mean velocity profiles to become similar and fully turbulent. Therefore, viscous effects across the entire turbulent mixing region will become important for long distances downstream of the present nonequilibrium shear layer.

CONCLUDING REMARKS

An experimental investigation of the initial development of turbulent free mixing at hypersonic speeds has been conducted. Mean profile data from conventional probes were obtained downstream of the exit of a Mach 19 nozzle in the initial free turbulent mixing layer and compared with similar data obtained previously in the nozzle-wall boundary layer. Also, at the same downstream station, the electron beam technique was used to measure both the mean density and static temperature across the shear layer. The results were obtained at a nominal total temperature of about 1670° K (3000° R) over a range of free-stream Reynolds number from 1.6×10^6 to 3.6×10^6 per meter (5×10^5 to 11×10^5 per foot).

A static-pressure gradient was present across the shear layer for the present tests. The outer 80 percent of the high-velocity portion of the initial free shear layer can be computed by a rotational method of characteristics. However, turbulent mixing is evidently important in the low-velocity region of the profiles and effects of eddy viscosity and eddy conductivity should be included in a theoretical analysis.

Langley Research Center,
National Aeronautics and Space Administration,
Hampton, Va., August 7, 1972.

REFERENCES

1. Pitkin, Edward T.; and Glassman, Irvin: Experimental Mixing Profiles of a Mach 2.6 Free Jet. J. Aerosp. Sci., vol. 25, no. 12, Dec. 1958, pp. 791-793.

2. Anderson, Arthur R.; and Johns, Frank R.: Characteristics of Free Supersonic Jets Exhausting Into Quiescent Air. Jet Propulsion, vol. 25, no. 1, Jan. 1955, pp. 13-15, 25.

3. Eggers, James M.: Velocity Profiles and Eddy Viscosity Distributions Downstream of a Mach 2.22 Nozzle Exhausting to Quiescent Air. NASA TN D-3601, 1966.

4. Lamb, J. P.: An Approximate Theory for Developing Turbulent Free Shear Layers. Paper No. 66-WA/FE-17, Amer. Soc. Mech. Eng., Nov.-Dec. 1966.

5. Heck, P. H.; and Ferguson, D. R.: Analytical Solution for Free Turbulent Mixing in Compressible Flows. AIAA Paper No. 71-4, Jan. 1971.

6. Vasiliu, John: Turbulent Mixing of a Rocket Exhaust Jet With a Supersonic Stream Including Chemical Reactions. J. Aerosp. Sci., vol. 29, no. 1, Jan. 1962, pp. 19-28.

7. Fox, Herbert; Sinha, Ram; and Weinberger, Lawrence: An Implicit Finite Difference Solution for Jet and Wake Problems. Pt. I: Analysis and Test Cases. ARL 70-0025, U.S. Air Force, Feb. 1970.

8. Clark, Frank L.; Ellison, James C.; and Johnson, Charles B.: Recent Work in Flow Evaluation and Techniques of Operations for the Langley Hypersonic Nitrogen Facility. Vol. I of Fifth Hypervelocity Techniques Symposium, Univ. of Denver, Mar. 1967, pp. 347-373. (Available from DDC as AD 819715.)

9. Beckwith, Ivan E.; Harvey, William D.; and Clark, Frank L. (With appendix A by Ivan E. Beckwith, William D. Harvey, and Christine M. Darden and appendix B by William D. Harvey, Lemuel E. Forrest, and Frank L. Clark): Comparisons of Turbulent-Boundary-Layer Measurements at Mach Number 19.5 With Theory and an Assessment of Probe Errors. NASA TN D-6192, 1971.

10. Yanta, William J.: A Hot-Wire Stagnation Temperature Probe. NOLTR 68-60, U.S. Navy, June 18, 1968.

11. Muntz, E. P.: The Electron Beam Fluorescence Technique. AGARDograph 132, Dec. 1968.

12. Hunter, William W., Jr.: Investigation of Temperature Measurements in 300° to 1100° K Low-Density Air Using an Electron Beam Probe. NASA TN D-4500, 1968.

13. Brinich, Paul F.; and Neumann, Harvey E.: Some Effects of Acceleration on the Turbulent Boundary Layer. AIAA J., vol. 8, no. 5, May 1970, pp. 987-989.

14. Dash, S.: An Analysis of Internal Supersonic Flows With Diffusion, Dissipation and Hydrogen-Air Combustion. ATL TR 152 (Contract NAS 1-9560), Advanced Technology Lab., Inc., May 1970. (Available as NASA CR-111783.)

15. Lillicrap, D. C.: Experimental Determination of Density and Rotational Temperature by an Improved Electron Beam Technique. AIAA Paper No. 71-605, June 1971.

16. Ashkenas, Harry: Rotational Temperature Measurements in Electron-Beam Excited Nitrogen. Phys. Fluids, vol. 10, no. 12, Dec. 1967, pp. 2509-2520.

17. Warren, Walter R., Jr.: The Static Pressure Variation in Compressible Free Jets. J. Aeronaut. Sci., vol. 22, no. 3, Mar. 1955, pp. 205-207.

TABLE I.- ACTUAL STAGNATION AND TEST CONDITIONS

$[T_W = T_B = 300^{\circ}K\ (540^{\circ}\ R)]$

Symbol	T_o		p_o		M_e	N_{Re}/m	N_{Re}/ft	p_e/p_o	p_W/p_o	p_B/p_o	ρ_e/ρ_o	x		Survey
	^{o}K	^{o}R	N/cm^2	lb/in^2								cm	in.	
○	1644	2960	2413	3500	19.34	1.62×10^6	4.96×10^5	0.264×10^{-6}	0.400×10^{-6}	0.195×10^{-6}	19.9×10^{-6}	238.1	93.75	Electron beam
[a]□◇	1644	2960	2413	3500	19.34	1.62	4.96	.264	.400	.195	19.9	238.1	93.75	Pitot, temp.
○	1658	2985	5585	8100	19.50	3.56	10.90	.249	.420	.149	19.2	238.1	93.75	Pitot, temp.
□	1667	3000	4320	6266	19.20	2.93	8.93	.277	.375	.213	20.7	238.1	93.75	Pitot, temp.
◇	1664	2995	4682	6791	19.20	2.38	7.26	.277	.355	.149	20.7	238.1	93.75	Static probe
— · —	1811	3260	4464	6475	19.40	2.04	6.23	.258	.400	.160	19.7	208.3	82.00	[b]Static probe
— —	1778	3200	4309	6256	19.40	2.02	6.20	.258	.390	.212	19.7	208.3	82.00	[b]Pitot, temp.
— ——	1833	3300	5585	8100	19.70	2.94	9.00	.232	.395	.150	18.3	208.3	82.00	[b]Pitot, temp.

[a]Figs. 2 and 3 only.

[b]Data from ref. 9.

TABLE II.- EXPERIMENTAL VALUES OF PITOT AND TOTAL TEMPERATURE FOR PROBES AT x = 2.381 m (93.75 in.)

(a) $N_{Re,x} = 8.52 \times 10^6$ and $M_e = 19.5$

y		p_{t_2}/p_o	y		T_t/T_o
cm	in.		cm	in.	
3.15	1.25	105.000×10^{-6}	4.32	1.70	1.000
3.68	1.45	101.500	5.21	2.05	1.000
4.56	1.80	101.500	5.89	2.32	1.000
5.21	2.05	101.400	6.65	2.62	1.000
5.84	2.40	109.000	7.41	2.92	1.000
6.86	2.70	108.000	8.18	3.22	1.000
7.75	3.05	112.000	9.19	3.62	1.000
8.38	3.30	119.000	10.03	3.95	.999
9.26	3.65	121.200	10.48	4.12	.990
9.90	3.90	120.300	11.07	4.35	.980
10.80	4.25	111.000	11.58	4.55	.965
11.41	4.50	101.000	12.25	4.82	.952
12.31	4.85	93.200	13.01	5.12	.931
13.31	5.25	78.500	13.76	5.41	.900
13.98	5.50	64.100	14.55	5.72	.865
14.85	5.85	51.000	15.30	6.02	.835
15.50	6.10	39.500	16.06	6.32	.800
16.62	6.55	30.500	16.81	6.62	.765
17.15	6.75	21.000	17.59	6.92	.710
17.90	7.05	12.900	18.31	7.21	.655
18.68	7.35	7.300	19.10	7.52	.610
19.41	7.65	4.100	19.95	7.85	.555
21.08	8.30	2.000	20.62	8.12	.490
21.60	8.50	1.260	21.50	8.45	.412
22.80	8.90	.755	22.18	8.72	.341
23.15	9.10	.450	23.00	9.05	.282
24.00	9.45	.300	23.75	9.35	.248
24.80	9.75	.220	25.20	9.91	.210
25.55	10.05	.180	25.98	10.21	.199
26.19	10.30	.169	26.76	10.52	.195
26.80	10.55	.159	27.30	10.75	.190
			27.00	11.02	.189

TABLE II.- EXPERIMENTAL VALUES OF PITOT AND TOTAL TEMPERATURE FOR PROBES AT x = 2.381 m (93.75 in.) – Concluded

(b) $N_{Re,x} = 6.97 \times 10^6$ and $M_e = 19.20$

y		p_{t_2}/p_o	y		T_t/T_o
cm	in.		cm	in.	
3.43	1.35	117.500×10^{-6}	4.70	1.85	1.000
4.19	1.65	125.000	5.64	2.22	1.000
4.95	1.95	125.000	6.65	2.62	1.000
5.46	2.15	117.500	7.83	3.08	1.000
5.96	2.35	117.000	8.69	3.42	1.000
6.35	2.50	121.000	9.45	3.72	1.000
6.86	2.70	121.000	9.95	3.92	1.000
7.36	2.90	126.000	10.45	4.12	.993
8.00	3.15	135.000	10.98	4.32	.982
8.50	3.35	137.500	11.72	4.62	.962
8.76	3.45	137.000	12.50	4.92	.942
9.40	3.70	133.600	13.00	5.12	.925
9.90	3.90	131.000	13.51	5.32	.912
10.41	4.10	115.000	14.01	5.52	.895
10.91	4.30	111.000	15.10	5.95	.855
12.08	4.75	96.500	15.55	6.12	.822
12.45	4.90	86.500	16.55	6.52	.770
12.97	5.10	78.000	17.08	6.72	.741
13.48	5.30	69.500	17.58	6.92	.715
13.99	5.50	60.000	18.10	7.12	.682
14.61	5.75	53.000	18.65	7.35	.675
15.11	5.95	45.000	19.19	7.55	.645
15.89	6.25	35.500	19.70	7.55	.578
17.15	6.75	21.900	20.02	7.95	.525
17.51	6.90	16.500	20.70	8.15	.475
18.06	7.10	11.600	20.98	8.25	.425
18.55	7.30	5.700	21.70	8.55	.375
19.20	7.55	5.190	22.20	8.75	.331
19.58	7.70	3.190	22.75	8.95	.295
20.05	7.90	2.400	23.20	9.15	.265
20.60	8.10	1.910	24.42	9.53	.225
21.06	8.30	1.450	25.78	10.12	.198
21.75	8.55	1.120	27.00	10.62	.191
22.10	8.70	.810	28.00	11.02	.189
22.60	8.90	.570			
23.10	9.10	.418			
24.62	9.70	.252			
25.50	10.05	.193			
26.65	10.50	.159			

TABLE III.- EXPERIMENTAL VALUES OF DENSITY AND TEMPERATURE FOR ELECTRON BEAM AT $x = 2.381$ m (93.75 in.)

$[N_{Re,x} = 3.88 \times 10^6$ and $M_e = 19.34]$

y		ρ/ρ_o
cm	in.	
0	0	18.70×10^{-6}
1.26	.50	18.30
2.54	1.00	18.20
3.81	1.50	18.30
5.08	2.00	18.50
6.35	2.50	17.85
7.61	3.00	17.30
8.25	3.25	16.80
8.90	3.50	16.20
9.52	3.75	15.50
10.15	4.00	14.20
11.41	4.50	12.90
12.70	5.00	11.20
13.99	5.50	8.90
15.25	6.00	5.80
16.50	6.50	3.40
17.80	7.00	2.10
19.05	7.50	1.50
20.30	8.00	1.05
21.60	8.50	1.30

x		$\bar{T}/T_o$
cm	in.	
0	0	0.0200
5.08	2.00	.0210
10.15	4.00	.0280
11.41	4.50	.0360
12.70	5.00	.0335
13.34	5.25	.0400
13.99	5.50	.0440
14.60	5.75	.0550
15.25	6.00	.0615
15.88	6.25	.0845
16.50	6.50	.0995
17.15	6.75	.1210
17.80	7.00	.1450
18.40	7.25	.1780
19.05	7.50	.2130
19.70	7.75	.2350
20.30	8.00	.2520
20.95	8.25	.2540
21.60	8.50	.2460
22.20	8.75	.2710
22.80	9.00	.2340

TABLE IV.- EXPERIMENTAL SHEAR FLOW PROFILES AT $x = 2.381$ m (93.75 in.)

(a) $N_{Re,x} = 8.52 \times 10^6$ and $M_e = 19.5$; $y_\delta = 9.15$ cm (3.6 in.); $\frac{p(y)}{p_o} = \frac{p_e}{p_o}$ (constant)

y		M/M_e	u/u_e	p/p_{t_2}	M
cm	in.				
9.195	3.62	1.000	1.000	2.0410×10^{-3}	19.50
10.033	3.95	.999	.999	2.0450×10^{-3}	19.48
10.465	4.12	.989	.993	2.0855×10^{-3}	19.36
11.049	4.35	.975	.990	2.1470×10^{-3}	19.31
11.557	4.55	.927	.985	2.3730×10^{-3}	18.08
12.243	4.82	.885	.980	2.6040×10^{-3}	17.26
13.005	4.12	.834	.965	2.9340×10^{-3}	16.26
13.741	5.41	.763	.940	3.5020×10^{-3}	14.88
14.529	5.72	.689	.919	4.2910×10^{-3}	13.44
15.291	6.02	.601	.895	5.6390×10^{-3}	11.72
16.053	6.32	.523	.875	7.4390×10^{-3}	10.20
16.815	6.62	.446	.839	1.0210×10^{-2}	8.70
17.577	6.92	.355	.791	1.6100×10^{-2}	6.92
18.313	7.21	.265	.732	2.8670×10^{-2}	5.17
19.101	7.52	.200	.663	4.9870×10^{-2}	3.90
19.939	7.85	.165	.600	7.2350×10^{-2}	3.22
20.625	8.12	.138	.518	$.1021 \times 10^{-2}$	2.69
21.463	8.45	.108	.421	$.1608 \times 10^{-2}$	2.11
22.149	8.72	.081	.312	$.2685 \times 10^{-2}$	1.58
22.987	9.05	.051	.215	$.5283 \times 10^{-2}$	.99
23.749	9.35	.035	.122	$.7338 \times 10^{-2}$	.68

(b) $N_{Re,x} = 6.97 \times 10^6$ and $M_e = 19.20$; $y_\delta = 9.4$ cm (3.7 in.); $\frac{p(y)}{p_o} = \frac{p_e}{p_o}$ (constant)

y		M/M_e	u/u_e	p/p_{t_2}	M
cm	in.				
9.449	3.72	1.000	1.000	0.2105×10^{-2}	19.20
9.957	3.92	.999	.999	$.2151 \times 10^{-2}$	18.99
10.465	4.12	.958	.996	$.2294 \times 10^{-2}$	18.39
10.973	4.32	.932	.990	$.2424 \times 10^{-2}$	17.89
11.735	4.62	.905	.985	$.2568 \times 10^{-2}$	17.38
12.497	4.92	.842	.970	$.2966 \times 10^{-2}$	16.17
13.005	5.12	.795	.965	$.3330 \times 10^{-2}$	15.26
13.513	5.32	.743	.950	$.3807 \times 10^{-2}$	14.27
14.021	5.52	.689	.935	$.4428 \times 10^{-2}$	13.23
15.113	5.95	.589	.910	$.6055 \times 10^{-2}$	11.31
15.545	6.12	.553	.882	$.6866 \times 10^{-2}$	10.62
16.561	6.52	.445	.841	$.1060 \times 10^{-1}$	8.54
17.069	6.72	.402	.815	$.1295 \times 10^{-1}$	7.72
17.577	6.92	.355	.791	$.1657 \times 10^{-1}$	6.82
18.085	7.12	.295	.755	$.2397 \times 10^{-1}$	5.66
18.669	7.35	.218	.721	$.4334 \times 10^{-1}$	4.19
19.177	7.55	.175	.620	$.6664 \times 10^{-1}$	3.36
19.685	7.75	.165	.600	$.7457 \times 10^{-1}$	3.17
20.193	7.95	.135	.535	$.1097 \times 10^{-1}$	2.59
20.701	8.15	.115	.473	$.1476 \times 10^{-1}$	2.21
20.955	8.25	.100	.408	$.1909 \times 10^{-1}$	1.92
21.717	8.55	.085	.341	$.2546 \times 10^{-1}$	1.63
22.225	8.75	.070	.275	$.3516 \times 10^{-1}$	1.34
22.733	8.95	.062	.221	$.4204 \times 10^{-1}$	1.19
23.241	9.15	.042	.165	$.6495 \times 10^{-1}$	.81

TABLE IV.- EXPERIMENTAL SHEAR FLOW PROFILES

AT x = 2.381 m (93.75 in.) – Concluded

(c) $N_{Re,x} = 5.65 \times 10^6$ and $M_e = 19.34$; $y_\delta = 9.4$ cm (3.7 in.);

$\frac{p(y)}{p_o} = \frac{p}{p_o}$ (electron beam)

y		M/M_e	u/u_e	p/p_{t_2}	M
cm	in.				
9.449	3.72	1.000	1.000	0.2074×10^{-2}	19.34
9.957	3.92	.998	.999	$.2083 \times 10^{-2}$	19.30
10.465	4.12	.973	.989	$.2191 \times 10^{-2}$	18.82
10.973	4.32	.960	.980	$.2250 \times 10^{-2}$	18.57
11.735	4.62	.945	.975	$.2321 \times 10^{-2}$	18.28
12.497	4.92	.905	.965	$.2533 \times 10^{-2}$	17.50
13.005	5.12	.872	.955	$.2729 \times 10^{-2}$	16.86
13.513	5.32	.808	.945	$.3174 \times 10^{-2}$	15.63
14.021	5.52	.773	.933	$.3469 \times 10^{-2}$	14.95
15.113	5.95	.631	.910	$.5205 \times 10^{-2}$	12.20
15.545	6.12	.645	.885	$.4983 \times 10^{-2}$	12.47
16.561	6.52	.525	.850	$.7513 \times 10^{-2}$	10.15
17.069	6.72	.493	.833	$.8518 \times 10^{-2}$	9.53
17.577	6.92	.445	.815	$.1043 \times 10^{-1}$	8.61
18.085	7.12	.405	.791	$.1259 \times 10^{-1}$	7.83
18.669	7.35	.315	.781	$.2074 \times 10^{-1}$	6.09
19.177	7.55	.252	.733	$.3226 \times 10^{-1}$	4.87
19.685	7.75	.225	.675	$.4027 \times 10^{-1}$	4.35
20.193	7.95	.178	.611	$.6367 \times 10^{-1}$	3.44
20.701	8.15	.158	.545	$.7982 \times 10^{-1}$	3.06
20.955	8.25	.133	.475	$.1113 \times 10^{-1}$	2.57
21.717	8.55	.116	.408	$.1440 \times 10^{-1}$	2.24
22.225	8.75	.091	.335	$.2228 \times 10^{-1}$	1.76
22.733	8.95	.076	.272	$.3029 \times 10^{-1}$	1.47
23.241	9.15	.059	.221	$.4467 \times 10^{-1}$	1.14

NASA-Langley, 1972 —— 12 L-8409

TIONAL AERONAUTICS AND SPACE ADMINISTRATION
WASHINGTON, D.C. 20546

OFFICIAL BUSINESS
PENALTY FOR PRIVATE USE $300

SPECIAL FOURTH-CLASS RATE
BOOK

POSTAGE AND FEES PAID
NATIONAL AERONAUTICS AND
SPACE ADMINISTRATION
451

U.S.MAIL

POSTMASTER: If Undeliverable (Section 158 Postal Manual) Do Not Return

"The aeronautical and space activities of the United States shall be conducted so as to contribute . . . to the expansion of human knowledge of phenomena in the atmosphere and space. The Administration shall provide for the widest practicable and appropriate dissemination of information concerning its activities and the results thereof."

—NATIONAL AERONAUTICS AND SPACE ACT OF 1958

NASA SCIENTIFIC AND TECHNICAL PUBLICATIONS

TECHNICAL REPORTS: Scientific and technical information considered important, complete, and a lasting contribution to existing knowledge.

TECHNICAL NOTES: Information less broad in scope but nevertheless of importance as a contribution to existing knowledge.

TECHNICAL MEMORANDUMS: Information receiving limited distribution because of preliminary data, security classification, or other reasons. Also includes conference proceedings with either limited or unlimited distribution.

CONTRACTOR REPORTS: Scientific and technical information generated under a NASA contract or grant and considered an important contribution to existing knowledge.

TECHNICAL TRANSLATIONS: Information published in a foreign language considered to merit NASA distribution in English.

SPECIAL PUBLICATIONS: Information derived from or of value to NASA activities. Publications include final reports of major projects, monographs, data compilations, handbooks, sourcebooks, and special bibliographies.

TECHNOLOGY UTILIZATION PUBLICATIONS: Information on technology used by NASA that may be of particular interest in commercial and other non-aerospace applications. Publications include Tech Briefs, Technology Utilization Reports and Technology Surveys.

Details on the availability of these publications may be obtained from:

SCIENTIFIC AND TECHNICAL INFORMATION OFFICE

NATIONAL AERONAUTICS AND SPACE ADMINISTRATION

Washington, D.C. 20546